Density dependent hadron field theory for hypernuclei

C. M. Keil, F. Hofmann, and H. Lenske

Institut für Theoretische Physik, Universität Gießen, Heinrich-Buff-Ring 16, 35392 Gießen, Germany

(Received 4 November 1999; published 12 May 2000)

The density dependent relativistic hadron field (DDRH) theory, previously introduced and applied to isospin nuclei, is extended to hypernuclei by including the octet hyperons. Infinite matter Dirac-Brueckner theory for octet baryons and the derivation of in-medium DDRH baryon-meson vertices is discussed. From the properties of Dirac-Brueckner interactions it is found that hyperon and nucleon self-energies and vertices are related by the ratios of free space coupling constants. This leads to simple scaling laws for the in-medium hyperon and nucleon vertices. The model is applied in relativistic DDRH mean-field calculations to single Λ nuclei. Free space $N\Lambda$ T-matrix results are used for the scalar vertex. As the only free parameter the hyperon vector vertex scaling factor is adjusted to a selected set of hypernuclear data. Spectroscopic data of single Λ hypernuclei over the full mass range are well described. A reduction of the Λ spin-orbit splitting is found to be related closely to the medium dependence of scalar and vector interactions.

PACS number(s): 21.80.+a

I. INTRODUCTION

Hypernuclei are unique in providing access to the dynamics of the full meson and baryon $SU(3)$ flavor octets. Their study is the natural extension of the isospin dynamics in nonstrange nuclei towards a more general theory of flavor dynamics in a baryonic environment. Obviously, from a QCD point of view hypernuclei are deep in the nonperturbative low energy-momentum regime, as are isospin nuclei. Hence, a description in terms of mesons and baryons should be adequate. Single Λ hypernuclei, produced in (K^-,π^-) or (π^+,K^+) reactions on a nuclear neutron are the best-studied examples. Their properties confirm that adding a unit of strangeness to an isospin nucleus indeed produces a system which, to a large extent, follows similar rules as isospin nuclei [1,2]. Such observations give strong evidence that the strangeness content of a hypernucleus is in fact stored in a hyperon. Moreover, hypernuclear spectroscopy indicates the existence of shell structures compatible with independent (quasi-)particle motion in a static mean field. The effective potential, however, is found to be considerably more shallow than for nucleons. A natural explanation for the reduction in depth to about 50% of the nucleon value is provided by assuming that the mean-field producing σ and ω meson fields are not coupled to strangeness. Under these ''ideal mixing'' conditions the meson-hyperon coupling should evolve according to the ratio of strange to nonstrange quarks in a baryon, i.e., a reduction of vertices by at least a factor of $R_{\sigma,\omega} \sim 2/3$ is expected for Λ and Σ hyperons. However, to account for the experimentally observed decrease of the spin-orbit splitting in Λ nuclei in such a quark counting model, it is necessary to introduce an additional quenching factor. Within a valence quark model, for example, the $\Lambda-\omega$ spin-orbit contribution is strongly reduced by introducing a $\Lambda-\omega$ tensor interaction [3–6].

Modern approaches to hypernuclear structure use nonrelativistic and relativistic microscopic descriptions. Relativistic mean-field (RMF) theories of Walecka-type [7] have been applied successfully [8–10] with empirically adjusted meson-hyperon vertices. $SU(3)_f$-symmetric field theories incorporating chirality [11,12] or accounting for the quark structure of hadrons [6,13] have been formulated and applied to hypernuclei. Extensions to still unobserved multistrangeness systems ($|S|>2$) have been explored and predict a gain of binding energy when adding a few units of strangeness to an isospin nucleus [8,14–16]. The production of strangelets in ultrarelativistic heavy ion collisions as a new form of hadronic matter has been postulated [17]. Using $SU(3)_f$ arguments nucleon-hyperon and hyperon-hyperon interactions in free space [18–20] and in a nuclear environment [21–23] were calculated.

In this paper, hypernuclei are described in the density dependent relativistic hadron (DDRH) theory, which was introduced previously as an effective field theory for isospin nuclei [24,25]. In DDRH theory the medium dependence of nuclear interactions is described by meson-nucleon vertices which are functionals of the fermion field operators. Lorentz invariance, thermodynamical consistency, and covariance of the field equations are retained. Taking the functional dependence of the vertices on density from infinite matter Dirac-Brueckner Hartree-Fock (DBHF) calculations a practically parameter free model Lagrangian is obtained once a free space nucleon-nucleon (NN) interaction is chosen.

A particular conceptual difference to other approaches is the DDRH treatment of nonlinearities in terms of invariants of fermion field operators. Since the baryon fields are treated as quantum fields even in the mean-field limit a well-defined class of quantum fluctuations with nonvanishing ground state expectation value is taken into account [25,26]. Dynamically, they contribute to the Dirac equations as rearrangement self-energies describing the static polarization of the medium. In standard relativistic mean-field (RMF) theory nonlinearities are attributed to higher order self-interactions of meson fields [27]. In a mean-field approximation, mesons are treated as classical fields and fluctuations around the classical field configurations are neglected by definition. In bulk quantities, as for example total binding energies, the differences of the DDRH and the RMF approach are hardly detectable because the DDRH rearrangement self-energies are cancelled exactly in extensive thermodynamical quantities

[25]. But in single particle quantities like separation energies, wave functions, and density matrices the differences become visible [25]. DDRH coupling constants in asymmetric matter [28] and modifications from vacuum polarization [29] have been investigated.

The extension of DDRH theory to strange baryons is discussed in Sec. II. The theoretical formulation is kept general allowing us to include the lowest SU(3) baryon and meson octets. For practical reasons, however, only strangeness-neutral meson fields are taken into account at present. As the central theoretical result we derive in Sec. II B scaling laws for in-medium hyperon vertices given by an almost density independent renormalization of the nucleon vertices through the ratios of free space coupling constants. In phenomenological RMF approaches [8,9,30], a similar scaling *ansatz* for the meson-Λ vertices is used but here it is obtained theoretically. Equations of motion and the Hartree mean-field limit are derived. In Sec. III a reduced model appropriate for single Λ nuclei is introduced. Since strangeness carrying mean fields can be neglected for single-Λ nuclei [they are of the order $\mathcal{O}(1/A)$, A being the mass number] the mean-field equations are considerably simplified. In the applications the σ coupling is taken from a theoretical $N\Lambda$ T matrix [18,31] while the ω coupling is determined empirically. DDRH mean-field results for hypernuclei are presented in Sec. IV and compared to data and conventional RMF calculations. Spectroscopic data are well described, showing also a reduced spin-orbit splitting in Λ nuclei. The paper closes with a summary and conclusions in Sec. V.

II. DENSITY DEPENDENT HADRON FIELD THEORY WITH HYPERONS

A. The model Lagrangian

The derivation of a symmetry-broken physical model from a $SU(3)_f$ Lagrangian has been exercised in the literature, e.g., in Ref. [32]. However, in order to describe nuclear structure phenomena for spin saturated and rotationally symmetric systems one finds that most of the $SU(3)_f$ structures are actually not contributing in RMF prescription. The reason is obvious because parity conservation inhibits the appearance of condensed pseudoscalar fields in this case. Hence, neither of the 0^- meson fields contributes directly to a hypernuclear calculation for the case of a single hyperon moving in the field of a 0^+-core nucleus. Those contributions of pseudoscalar mesons are *not* simply neglected in the calculations (since they are fairly important) but rather taken into account effectively via the modified in-medium couplings (see Sec. II B). From the 1^- vector meson octet condensed isoscalar ω and isovector ρ meson fields will evolve. In a system with a large fraction of hyperons condensed octet K^* fields can also appear. However, an apparent shortcoming of a pure $SU(3)_f$ approach is the missing scalar mesons and, hence, absence of a binding mean field. A satisfactory description of the 0^+ meson channels, e.g., in terms of dynamical two-meson correlations [18,31], is an unsolved question.

Here we follow the line of relativistic mean-field theory [7] and restrict the model to the degrees of freedom which are relevant for the nuclear structure problem. In practice, we use the DDRH Lagrangian [25] which is extended in the baryon sector by including the lowest $S=-1$ (Λ,Σ) and $S=-2$ (Ξ) baryons. We introduce the flavor spinor Ψ_F

$$\Psi_F=(\Psi_N,\Psi_\Lambda,\Psi_\Sigma,\Psi_\Xi)^T, \tag{1}$$

composed of the isospin multiplets

$$\Psi_N=\begin{pmatrix}\psi_p\\\psi_n\end{pmatrix}, \quad \Psi_\Lambda=\psi_\Lambda,$$

$$\Psi_\Sigma=\begin{pmatrix}\psi_{\Sigma^+}\\\psi_{\Sigma^0}\\\psi_{\Sigma^-}\end{pmatrix}, \quad \Psi_\Xi=\begin{pmatrix}\psi_{\Xi^0}\\\psi_{\Xi^-}\end{pmatrix}, \tag{2}$$

where ψ_i are Dirac spinors. The full Lagrangian is structured in an isospin symmetric way. In the exchange particle sector the isoscalar σ, σ_s ($\equiv$scalar $s\bar{s}$ condensate), ω and ϕ meson, the isovector ρ meson, and the photon γ are included. This leads to the Lagrangian

$$\mathcal{L}=\mathcal{L}_B+\mathcal{L}_M+\mathcal{L}_{\text{int}}$$

$$\mathcal{L}_B=\bar{\Psi}_F[i\gamma_\mu\partial^\mu-\hat{M}]\Psi_F$$

$$\mathcal{L}_M=\frac{1}{2}\sum_{i=\sigma,\sigma_s}(\partial_\mu\Phi_i\partial^\mu\Phi_i-m_i^2\Phi_i^2)$$

$$-\frac{1}{2}\sum_{\kappa=\omega,\phi,\rho,\gamma}\left(\frac{1}{2}F^{(\kappa)^2}-m_\kappa^2 A^{(\kappa)^2}\right) \tag{3}$$

$$\mathcal{L}_{\text{int}}=\bar{\Psi}_F\hat{\Gamma}_\sigma(\bar{\Psi}_F,\Psi_F)\Psi_F\sigma-\bar{\Psi}_F\hat{\Gamma}_\omega(\bar{\Psi}_F,\Psi_F)\gamma_\mu\Psi_F\omega^\mu$$

$$-\frac{1}{2}\bar{\Psi}_F\hat{\vec{\Gamma}}_\rho(\bar{\Psi}_F,\Psi_F)\gamma_\mu\Psi_F\vec{\rho}^\mu+\bar{\Psi}_F\hat{\Gamma}_{\sigma_s}(\bar{\Psi}_F,\Psi_F)\Psi_F\sigma_s$$

$$-\bar{\Psi}_F\hat{\Gamma}_\phi(\bar{\Psi}_F,\Psi_F)\gamma_\mu\Psi_F\phi^\mu-e\bar{\Psi}_F\hat{Q}\gamma_\mu\Psi_F A^\mu,$$

where $\mathcal{L}_B$ and $\mathcal{L}_M$ are the free baryonic and mesonic Lagrangians, respectively, and the meson-baryon interactions are contained in $\mathcal{L}_{\text{int}}$. The diagonal matrix $\hat{M}$ contains the free-space baryon masses, and

$$F_{\mu\nu}^{(\kappa)}=\partial_\mu A_\nu^{(\kappa)}-\partial_\nu A_\mu^{(\kappa)} \tag{4}$$

is the field strength tensor of either the vector mesons ($\kappa=\omega,\phi,\rho$) or the photon ($\kappa=\gamma$). In Eq. (3) contractions of the field strength tensors are abbreviated as $F^2=F_{\mu\nu}F^{\mu\nu}$, etc. $\hat{Q}$ is the electric charge operator. σ_s and Φ meson fields are included mainly for reasons of completeness. The corresponding classical, condensed fields will be important only when treating systems with more than one unit of strangeness. Already in $\Lambda-\Lambda$-nuclei strange mesons should be included to reproduce the empirical strongly attractive pairing-force between Λ's [33]. For single Λ nuclei, however, they should be negligible [$\mathcal{O}(1/A)$]. Lagrangians of a similar

structure, but with constant meson-baryon vertices, are used successfully in relativistic mean-field calculations of hypernuclei, see, e.g., [8,9].

An isospin symmetric interaction is obtained with vertices chosen as

$$(\hat{\Gamma}_\alpha)_{BB'} = \Gamma_{\alpha B}\delta_{BB'}, \quad \alpha = \sigma, \sigma_s, \omega, \phi$$

$$(\hat{\vec{\Gamma}}_\rho)_{BB'} = \vec{\Gamma}_{\rho B}\delta_{BB'}, \quad \vec{\Gamma}_{\rho B} = \Gamma_{\rho B}\vec{\tau}_B$$

$$\text{for} \quad B, B' = N, \Lambda, \Sigma, \Xi, \quad (5)$$

where $\vec{\tau}^B$ are the isospin Pauli matrices. In DDRH theory the vertices $\Gamma_{\alpha B} = \Gamma_{\alpha B}(\bar{\Psi}, \Psi)$ are taken as functionals of the baryon field operators [24,25].

B. Baryon-baryon vertices from Dirac-Brueckner theory

In order to understand the subtleties of including baryon-baryon (BB) correlations in a field theory of a higher flavor content we briefly sketch the derivation of the vertices Γ from Dirac-Brueckner theory. The main outcome of the discussions is that nucleon and hyperon dynamics should be related to a good approximation by simple scaling laws.

A Lagrangian of the type defined above leads to a ladder kernel $V^{BB'}(q',q)$ given in momentum representation by the superposition of one boson exchange (OBE) potentials $V_\alpha^{BB'}(q',q)$. The latter are Lorentz invariants,

$$V_\alpha^{BB'}(q',q) = g_{\alpha B}g_{\alpha B'}D_\alpha(t)\langle \bar{u}^{B_1}(q')\kappa_\alpha u^{B_3}(q)\rangle$$

$$\cdot \langle \bar{u}^{B'_2}(-q')\kappa^\alpha u^{B'_4}(-q)\rangle, \quad (6)$$

where $t = (q'-q)^2$ is the four-momentum transfer, and κ_α denotes the Dirac and flavor structure of the vertex with bare coupling constants $g_{\alpha B}$ and $g_{\alpha B'}$ for baryons B and B' belonging to different isospin multiplets. The Dirac spinors are indicated by $u^B(q)$. Contractions over Dirac and flavor indices are indicated by the notation $\kappa_\alpha \cdot \kappa^\alpha$. At this point the full spectrum of octet-mesons should be taken into account—irrespective of whether they lead to condensed classical fields or not—because we are dealing with the in-medium BB'-scattering amplitudes. Working in the BB' center-of-momentum frame q and q' denote the relative four-momenta in the in- and outgoing channels (B_3, B'_4) and (B_1, B'_2), respectively, where $-q = (q_0, -\mathbf{q})$.

Solving the Bethe-Salpeter equation with the kernel $V^{BB'} = \Sigma_\alpha V_\alpha^{BB'}$

$$\mathcal{R}^{BB'}(q',q) = V^{BB'}(q',q) + \int dk\, V^{BB'}(q',k)Q_F^{BB'}(k,q)$$

$$\times \mathcal{R}^{BB'}(k,q) \quad (7)$$

leads to the in-medium interactions $\mathcal{R}^{BB'} = \langle k_1^B(q')k_2^{B'}(-q')|\mathcal{R}(k_F^B, k_F^{B'})|k_3^B(q)k_4^{B'}(-q)\rangle$. The Pauli-projected intermediate two-particle propagation, denoted by $GQ_F(BB')$, introduces an intrinsic dependence on the Fermi

momenta ($k_F^B, k_F^{B'}$). Dependencies on the (conserved) total center-of-mass energy $s = (k_3^B + k_4^{B'})^2$ are implicit. Evaluating Eq. (7) with self-consistent in-medium spinors, including the self-energies $\Sigma^B(k)$, introduces additional medium dependencies.

In structure calculations the G matrices $\mathcal{R}^{BB'}$ are required in the nuclear matter rest frame rather than in the two-body c.m. system. In practice, the transformation is achieved by projection on the standard set of scalar (S), vector (V), tensor (T), axial vector (A), and pseudoscalar (P) Lorentz invariants [34–36]. For our purpose, however, a more convenient representation is obtained by forming appropriate linear combinations of the so obtained coefficients and to map the set (S,V,T,A,P) onto the vertices of OBE interactions, Eq. (6). This allows us to express the (BB') G matrices, Eq. (7), in terms of renormalized OBE interactions,

$$\mathcal{R}_\alpha^{BB'}(q',q) = z_\alpha^{BB'}(s,t,u|k_F^B k_F^{B'})g_{\alpha B}g_{\alpha B'}D_\alpha(t)$$

$$\times \langle \bar{u}^{B_1}(q')\kappa_\alpha u^{B_3}(q)\rangle$$

$$\cdot \langle \bar{u}^{B'_2}(-q')\kappa^\alpha u^{B'_4}(-q)\rangle. \quad (8)$$

The vertex invariants have been decomposed further into boson propagators $D_\alpha(t)$ and renormalization coefficients $z^{BB'}$ which both are Lorentz invariants. From this representation it is apparent that correlations are shifted into the vertex factors $z^{BB'}$. In principle, they may depend on the full set of Mandelstam variables s, t, and u and the Fermi momenta of baryons B and B'. However, most of the t dependence is already accounted for by the meson propagator $D_\alpha(t)$ and considering the mild variation of DB G matrices on the center-of-mass energy the z coefficients can be expected to depend mainly on the Fermi momenta. If necessary, the u dependence can be removed to a large extent by adding a term proportional to $D_\alpha(u)$, i.e., introducing antisymmetrization explicitly. Note that antisymmetrization effects contribute only to states within the same isospin multiplet, i.e., $B = B'$. The self-energy of baryon B, however, includes contributions from all multiplets:

$$\langle \bar{u}^B(k)\kappa^\alpha u^B(k)\rangle\Sigma_\alpha^B(k|k_F)$$

$$= \sum_{B'} \int_{K_F^{B'}} d^4q[\text{Tr}(\langle k^B q^{B'}|\mathcal{R}^{BB'}|k^B q^{B'}\rangle S_F^{B'}(q))$$

$$+ \delta_{BB'}\langle k^B q^{B'}|\mathcal{R}^{BB'}|q^B k^{B'}\rangle S_F^{B'}(q)], \quad (9)$$

where the spacelike integration extends over the Fermi spheres $K_F^{B'}$ of baryons B' with in-medium (positive energy) propagators $S_F^{B'}(q)$ and $k_F = (k_F^N, k_F^Y)$ denotes the set of nucleon and hyperon Fermi momenta.

A particularly appealing aspect of Eq. (8) is that the z coefficients can be considered as medium-dependent renormalization factors of the OBE vertices. Exploiting the fact that the $SU(3)_f$ isospin multiplets are not mixed by strong interactions we are allowed to assume separability

$$z_\alpha^{BB'}(k,q|k_F^B,k_F^{B'}) \simeq s_\alpha^B(k_F^B)s_\alpha^{B'}(k_F^{B'}), \qquad (10)$$

and to neglect the (weak) residual momentum dependence. As a consequence,

$$g_{\alpha B}z_\alpha^{BB'}(k,q)g_{\alpha B'} \simeq \Gamma_{\alpha B}(k_F^B)\Gamma_{\alpha B'}(k_F^{B'}) \qquad (11)$$

where

$$\Gamma_{\alpha B}(k_F^B) \equiv g_{\alpha B}s_\alpha^B(k_F^B) \qquad (12)$$

defines the renormalized in-medium vertices in the ladder approximation. We introduce the antisymmetrized condensed Dirac Hartree-Fock (DHF) meson fields

$$\phi_\alpha(k|k_F,\Gamma) = \sum_{B'} \Gamma_{\alpha B'}D_\alpha(0)$$
$$\times \int_{K_F^{B'}} dq\, \mathrm{Tr}(\langle \bar{u}^{B'}(q)\kappa_\alpha u^{B'}(q)\rangle)$$
$$+ \sum_\mu \int_{K_F^B} dq f_{\alpha\mu}\Gamma_{\mu B}D_\mu(k-q)$$
$$\times \langle \bar{u}^B(q)\kappa_\alpha u^B(q)\rangle, \qquad (13)$$

where $f_{\alpha\mu}$ denotes the Fierz matrix [35,37] and $\Gamma = (\Gamma^N,\Gamma^Y)$. With our choice of momentum independent, global vertices, Eq. (9) takes then the approximate form

$$\Sigma_\alpha^B(k|k_F^N,k_F^Y) \simeq \Gamma_{\alpha B}(k_F^B)\phi_\alpha(k|k_F^N,k_F^Y,\Gamma). \qquad (14)$$

This equation establishes the link to the DDRH Lagrangian: In the DHF approximation self-energies of the same structure are obtained from Eq. (3). Comparing Eq. (13) and Eq. (14) it is also seen that strange and pseudoscalar mesons contribute only via the u-channel exchange diagrams to the self-energies in a parity conserving and time-reversal invariant system. A distinct role, however, is played by the mean-field producing 0^+ and 1^- mesons because they give rise to condensed classical fields in the ground state. Hence, at this stage we reduce the meson spectrum to the 0^+ and 1^- subset. This implies a redefinition of the $\alpha = \sigma,\omega,\rho,\delta$ vertex functions as indicated by Eq. (14).

In order to derive a self-contained model we apparently have to introduce a ''renormalization'' scheme. This is achieved by choosing symmetric hypermatter, i.e., $k_F^N = k_F^Y = k_F$. Writing down for that case Eq. (14) for nucleons and hyperons explicitly one finds

$$\Gamma_{\alpha Y}(k_F^Y) = \Gamma_{\alpha N}(k_F^Y)\frac{\Sigma_\alpha^Y(k|k_F)}{\Sigma_\alpha^N(k|k_F)}\bigg|_{k=k_F, k_F^N=k_F^Y}, \qquad (15)$$

which is exact in Hartree approximation. The above relation is the central result of this section. The obvious medium dependencies introduced in Eqs. (9) and (14) by the external baryon lines are eliminated such that the intrinsic medium properties of the underlying interactions are projected out. This is seen more clearly by considering the diagrammatic

structure of the DB self-energies [34,35]. The leading order (Hartree) contribution is given by tadpole diagrams and from a perturbation series expansion in the bare coupling constants $g_{\alpha B}$

$$R_\alpha^Y = \frac{\Sigma_\alpha^Y}{\Sigma_\alpha^N} \simeq \frac{g_{\alpha Y}}{g_{\alpha N}}\left(1+\mathcal{O}\left(1-\frac{M_N}{M_Y}\right)\right)+\cdots, \qquad (16)$$

where the realistic case $g_{\alpha Y} < g_{\alpha N}$ is considered. Hence, the R_α^Y are expected to be state-independent, universal constants whose values are close to the ratios of the bare coupling constants. For asymmetric matter with a hyperon fraction $\zeta_Y = \rho^Y/\rho^N \ll 1$ a corresponding diagrammatic analysis shows that asymmetry terms are in fact suppressed because the asymmetry correction is of leading second order $\mathcal{O}[((g_Y/g_N)\zeta_Y)^2]$. Thus, even in a finite nucleus where ζ_Y may vary over the nuclear volume, we expect $R_\alpha^Y = \mathrm{const}$ to a very good approximation.

In fact, these results agree with the conclusions drawn from the analysis of single hypernuclei in the past. In the present context, Eqs. (15) and (16) are of particular interest because they allow us to extend the DDRH approach in a theoretically meaningful way to hypernuclei using the results available already from the previous investigations of systems without strangeness. In the applications discussed below the nucleon (Hartree) scalar and vector vertex functions $\Gamma_{\sigma,\omega N}(k_F)$ of [25] will be used. The hyperon scaling factors R_α^Y are treated as phenomenological constants to be determined empirically. In the scalar channel information on R_σ^Y available from recent calculations of the Jülich group for the free $N\Lambda$ T matrix [18,31] is taken into account leaving essentially the ratio R_ω^Y/R_σ^Y for $Y = \Lambda$ as the only free parameter.

We close this section by remarking that Eq. (14) actually defines a set of quadratic equations for the vertices $\Gamma_{\alpha B}$, as seen immediately when inserting Eq. (13) into Eq. (14). Vertices derived in this way would be appropriate for DDRH calculations in Dirac-Hartree Fock approximation. From the $\sigma-\omega$ model it is known that DHF and relativistic Hartree calculations give almost indistinguishable results for properly adjusted parameters [7]. In the following we take advantage of that observation and, as in [25], restrict the calculations to the Hartree case only. This corresponds to determining the DDRH vertices by expressing the Φ_α fields on the right-hand side of Eq. (14) in Hartree approximation.

C. The equations of motion

In DDRH theory the above results are embedded into a relativistically covariant and thermodynamically consistent field theory from which the vertices are retrieved when evaluated in mean-field approximation. As discussed in [25] the k_F dependence of the DB vertices is expressed in terms of Lorentz-scalar (products of) bilinear forms $\hat{\rho}$ of the baryonic field operators Ψ_F. This provides a unique mapping of the medium dependence onto frame-independent Lorentz scalar quantities. The external Dirac structure of the vertices is fully determined by the Lorentz character of the meson

field. The intrinsic density dependence must be deduced from microscopic calculations as discussed in the previous section. As an obvious generalization of the *ansatz* used in [25] the DDRH vertices are expressed here as

$$\Gamma = \Gamma_{\alpha B}(\hat{\rho}_{\alpha B}(\bar{\Psi}_F, \Psi_F)),$$

$$\alpha = \sigma, \sigma_s, \omega, \phi, \rho, \quad B = N, \Lambda, \Sigma, \Xi, \quad (17)$$

where $\hat{\rho}_{\alpha B}$ denotes a Lorentz-scalar combination of the baryon field operators.

By definition the DB vertices $\Gamma^{DB}_{\alpha B}(k_F)$ are c-number valued functions of the Hartree or Hartree-Fock expectation value of $\hat{\rho}^{DB}_{\alpha B}$. From a general theoretical point of view the DDRH vertices $\Gamma_{\alpha B}(\hat{\rho}_{\alpha B})$ are not necessarily restricted to this particular subclass of diagrams. Formally, a projection onto DB correlations is defined by the mapping [25]

$$\Gamma_{\alpha B}(\hat{\rho}_{\alpha B}) = \int_0^\infty \Gamma^{DB}_{\alpha B}(\hat{\rho}^{DB}_{\alpha B}) \delta(\hat{\rho}^{DB}_{\alpha B} - \hat{\rho}_{\alpha B}) d\hat{\rho}^{DB}_{\alpha B}. \quad (18)$$

In the following a straightforward extension of the vector density dependence (VDD) prescription of Ref. [25] will be used. This corresponds to the *ansatz*

$$\hat{\rho}_{\alpha B}[\bar{\Psi}_F, \Psi_F] = \bar{\Psi}_F \hat{B}^{\alpha B}_\mu \gamma^\mu \Psi_F, \quad (19)$$

and chosing $(\hat{B}^{\alpha B}_\mu)_{B'B''} = u^B_\mu \delta_{BN} \delta_{B'N} \delta_{B''N}$ with u^B_μ a four-velocity (see [25]). We thus find $\hat{\rho}_{\alpha B} = \sqrt{j^B_\mu j^{B\mu}}$ and by means of Eq. (18) a Taylor series expansion of the DDRH vertex in terms (of the modulus) of only the respective baryon four-vector current is obtained. Exactly that choice of $\hat{B}^{\alpha B}_\mu$ is a practical implementation of the results obtained in Sec. II B. This shows that the DDRH approach in fact corresponds to expressing many-body correlations by an expansion of vertices into baryon n-point functions chosen such that in ground state expectation values correlation diagrams of the fully interacting theory are cancelled by compensating terms in the DDRH expansion.

As pointed out already in Ref. [25] the most important difference between DDRH and RMF theory is contributions from rearrangement self-energies to the DDRH baryon field equations. Rearrangement self-energies account physically for static polarization effects in the nuclear medium, cancelling certain classes of particle-hole diagrams [26]. Due to the additional strangeness degree of freedom the structure of these rearrangement self-energies is much more complex than in the purely nucleonic DDRH theory. The variational derivative of $\mathcal{L}_{\mathrm{int}}$ now leads to

$$\frac{\delta \mathcal{L}_{\mathrm{int}}}{\delta \bar{\Psi}_F} = \frac{\partial \mathcal{L}_{\mathrm{int}}}{\partial \bar{\Psi}_F} + \sum_{\substack{\alpha = \sigma, \sigma_s, \omega, \phi, \rho \\ B = N, \Lambda, \Sigma, \Xi}} \frac{\partial \mathcal{L}_{\mathrm{int}}}{\partial \hat{\rho}_{\alpha B}} \frac{\delta \hat{\rho}_{\alpha B}}{\delta \bar{\Psi}_F}. \quad (20)$$

With $S^{(r)\alpha B} \equiv \partial \mathcal{L} / \partial \hat{\rho}_{\alpha B}$ one finds

$$S^{(r)\alpha B} = \bar{\Psi}_F \frac{\partial \hat{\Gamma}_\alpha(\bar{\Psi}_F, \Psi_F)}{\partial \hat{\rho}_{\alpha B}} \Psi_F \Phi^\alpha$$

$$= \frac{\partial \Gamma_{\alpha B}(\hat{\rho}_{\alpha B})}{\partial \hat{\rho}_{\alpha B}} \Phi^\alpha \hat{\rho}^B_s, \quad \alpha = \sigma, \sigma_s, \quad (21)$$

$$S^{(r)\alpha B} = \bar{\Psi}_F \frac{\partial \hat{\Gamma}_\alpha(\bar{\Psi}_F, \Psi_F)}{\partial \hat{\rho}_{\alpha B}} \gamma^\mu \Psi_F \Phi^\alpha_\mu$$

$$= \frac{\partial \Gamma_{\alpha B}(\hat{\rho}_{\alpha B})}{\partial \hat{\rho}_{\alpha B}} \Phi^\alpha_\mu \hat{j}^\mu_B, \quad \alpha = \omega, \rho, \phi, \quad (22)$$

where $\hat{j}^B_\mu$ and $\hat{\rho}^B_s$ are the vector current operator and the scalar density operator of baryon type B, respectively. The rearrangement self-energy thus is given by

$$\hat{\Sigma}^{(r)} = \hat{\Sigma}^{(r)}_\mu \gamma^\mu, \quad (23)$$

$$\hat{\Sigma}^{(r)}_\mu = -\sum_{\alpha, B} S^{(r)\alpha B} \hat{B}^{\alpha B}_\mu, \quad (24)$$

where the sums in Eq. (24) are those appearing in Eq. (20). The usual self-energies [7] are given through

$$\hat{\Sigma}^{(0)}_s = \hat{\Gamma}_\sigma \sigma + \hat{\Gamma}_{\sigma_s} \sigma_s, \quad (25)$$

$$\hat{\Sigma}^{(0)\mu} = \hat{\Gamma}_\omega \omega^\mu + \hat{\Gamma}_\phi \phi^\mu + \hat{\vec{\Gamma}}_\rho \vec{\rho}^\mu + e\hat{Q} A^\mu, \quad (26)$$

where the $\hat{\Gamma}_\Phi$ are those defined in Eq. (5). Thus, the total baryon self-energies are finally obtained as

$$\hat{\Sigma}_s = \hat{\Sigma}^{(0)}_s, \quad \hat{\Sigma}^\mu = \hat{\Sigma}^{(0)\mu} + \hat{\Sigma}^{(r)\mu}. \quad (27)$$

Here, the $\hat{\Gamma}_\alpha$ are diagonal matrices containing the flavor dependent vertices. However, in structure the baryon field equations remain unchanged

$$[\gamma_\mu(i\partial^\mu - \hat{\Sigma}^\mu) - (\hat{M} - \hat{\Sigma}_s)] \Psi_F = 0. \quad (28)$$

D. Mean-field theory

A solvable model is obtained in the Hartree mean-field approximation which amounts to assuming that products of fermion operators are normal ordered with respect to the Hartree ground state $|0\rangle$, given by a single Slater determinant of occupied fermion states. Expectation values with respect to the Hartree ground state will be abbreviated as $\langle \hat{O} \rangle \equiv \langle 0|\hat{O}|0\rangle$. In the Hartree approach the vertex functionals $\Gamma_{\alpha B}(\hat{\rho}_{\alpha B})$ can be treated in a particularly simple way. Applying Wick's theorem one gets [25]

$$\langle \Gamma_{\alpha B}(\hat{\rho}_{\alpha B}) \rangle = \Gamma_{\alpha B}(\rho_{\alpha B}), \quad \rho_{\alpha B} \equiv \langle \hat{\rho}_{\alpha B} \rangle, \quad (29)$$

which brings the originally highly nonlinear field equations into a tractable form. Correspondingly the rearrangement contributions are obtained as

$$\left\langle \frac{\partial \Gamma_{\alpha B}(\hat{\rho}_{\alpha B})}{\partial \hat{\rho}_{\alpha B}} \right\rangle = \frac{\partial \Gamma_{\alpha B}(\rho_{\alpha B})}{\partial \rho_{\alpha B}}. \tag{30}$$

In the approximation as static classical fields the meson field equations reduce to

$$(-\nabla^2 + m_\alpha^2)\Phi_\alpha = \sum_{B=N,\Lambda,\Sigma,\Xi} \Gamma_{\alpha B}(\rho_{\Phi_\alpha B})\rho_s^B, \quad \alpha = \sigma, \sigma_s, \tag{31}$$

$$(-\nabla^2 + m_\alpha^2)\Phi_\alpha^\mu = \sum_{B=N,\Lambda,\Sigma,\Xi} \Gamma_{\alpha B}(\rho_{\Phi_\alpha B})j^{B\mu}, \quad \alpha = \omega, \phi, \tag{32}$$

$$(-\nabla^2 + m_\rho^2)\vec{\rho}^\mu = \sum_{B=N,\Lambda,\Sigma,\Xi} \vec{\Gamma}_{\rho B}(\rho_{\rho B})\vec{j}^{B\mu}. \tag{33}$$

The Dirac equation for the baryons remains the only equation of motion for an operator field, with dynamics given now by static but density-dependent self-energies

$$[\gamma_\mu(i\partial^\mu - \hat{\Sigma}^\mu(\rho)) - (\hat{M} - \hat{\Sigma}_s)]\Psi_F^{MF} = 0. \tag{34}$$

In finite nuclei, where $\rho = \rho(\mathbf{r})$, $\Sigma(\rho) = \Sigma(\mathbf{r})$ depends on the spatial coordinates.

III. THE $\Lambda - N$ MODEL

In order to test the scaling relation derived in Sec. II on existing hypernuclear data a model with Λ hyperons and nucleons interacting only by nonstrange mesons will be discussed. Naive quark counting suggests that even for $\Lambda-\Lambda$ interactions the strange mesons only contribute about 10% of the interaction strength. Since empirical results strongly contradict this estimate [33] and experimental data are deficient for determining, e.g., $\Gamma_{\phi B}$ and $\Gamma_{\sigma_s B}$ in a satisfactory way we will restrict ourselves to single-Λ nuclei. Keeping in mind the large uncertainties in the hyperon-nucleon and hyperon-hyperon interactions the exchange of strange mesons can be safely absorbed in the $\Lambda-\sigma$ and the $\Lambda-\omega$ vertices in this case. We will use the extended VDD prescription introduced in Sec. II C with a density-independent $N-\rho$ coupling, which leads to rather satisfactory results for isospin nuclei [25].

A. Λ-meson interaction

Due to the simple interaction structure of Λ hyperons— the Λ's are isoscalar and electrically neutral and thus couple neither to the ρ meson nor to the Coulomb field—the investigation of the Λ–nucleon interaction becomes rather transparent in this model. Assuming that the σ_s and the ϕ meson are pure $s\bar{s}$-states and therefore mainly couple to the strange

quark (due to OZI suppression), they will have no significant effect in single-Λ hypernuclei and can thus be safely neglected.

According to Sec. II B the density dependent vertices for the $\Lambda - N$ model are given by

$$\Gamma_{\sigma\Lambda} = R_\sigma \cdot \Gamma_{\sigma N}(\hat{\rho}_\Lambda),$$

$$\Gamma_{\omega\Lambda} = R_\omega \cdot \Gamma_{\omega N}(\hat{\rho}_\Lambda),$$

$$\hat{\rho}_\Lambda = \hat{\rho}_{\sigma\Lambda} = \hat{\rho}_{\omega\Lambda} = \sqrt{\hat{j}_\mu^\Lambda \hat{j}^{\Lambda\mu}}, \tag{35}$$

where $R_{\sigma,\omega}$ from now on denotes $R_{\sigma,\omega}^\Lambda$. The values for $R_{\sigma,\omega}$ will be determined in Sec. III C. The parametrizations of the nucleon-meson vertices $\Gamma_{iN}(\hat{\rho}_N)$ are taken from [38]. Numerically a fit with a second order polynomial in k_F to the vertices derived in [39] from nuclear matter DBHF self-energies is used.

B. Λ rearrangement dynamics

The considerations of Sec. III A define the dynamics of the Λ-nucleon system, i.e., the usual and the rearrangement self-energies can now be specified. Going to the nuclear rest frame, the arguments of the vertex functionals, $\hat{\rho}_{\alpha B}$, are now defined as in Eq. (19) with

$$\hat{B}_\mu^B = \hat{B}_\mu^{\sigma B} = \hat{B}_\mu^{\omega B} = \begin{pmatrix} \hat{u}_\mu^N \delta^{NB} & 0 \\ 0 & \hat{u}_\mu^\Lambda \delta^{\Lambda B} \end{pmatrix} \tag{36}$$

and $\hat{u}_\mu = (1,0,0,0)$. This leads to the rearrangement self-energy

$$\hat{\Sigma}_\mu^{(r)} = \sum_{B=N,\Lambda} \bar{\Psi}_F \left[\frac{\partial \hat{\Gamma}_\sigma}{\partial \hat{\rho}_{\sigma B}} \sigma - \frac{\partial \hat{\Gamma}_\omega}{\partial \hat{\rho}_{\omega B}} \gamma_\nu \omega^\nu \right] \Psi_F \hat{B}_\mu^B, \tag{37}$$

where the nucleon and Λ parts are given explicitly by

$$\Sigma_\mu^{(r)B} = \left[\frac{\partial \Gamma_{\sigma B}(\hat{\rho}_0^B)}{\partial \hat{\rho}_0^B} \sigma \hat{\rho}_s^B - \frac{\partial \Gamma_{\omega B}(\hat{\rho}_0^B)}{\partial \hat{\rho}_0^B} \omega^\nu \hat{j}_\nu^B \right] u_\mu^B \tag{38}$$

and $B = N, \Lambda$ vertices depend intrinsically only on their own densities, as derived in Sec. II B.

C. The vertex scaling factors

A consistent extension of the DDRH theory to strangeness requires using vertex functionals from DB self-energies calculated in the complete octet sector. However, since such a full scale calculation is neither available nor feasible under the present conditions, we choose a semiempirical approach combining existing theoretical information on the $\Lambda-\sigma$ vertex with a phenomenological description of the ω vertex scaling factor.

Actually, an extension of the Bonn potential to the free $N-\Lambda$ system already exists [18,31], but DB calculations are pending. We use the extended Bonn-A potential as a guide-
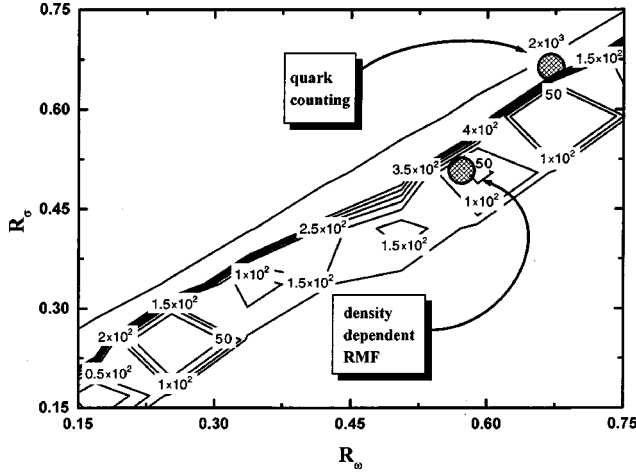
FIG. 1. χ^2 distribution for the deviation of DDRH Λ single particle energies and hypernuclear data (obtained in (π,K) reactions [40–44]). In the calculations, the scalar and vector vertex factors (R_σ, R_ω) were varied freely.

line to determine the relative couplings R_σ and R_ω. This is consistent with the approach used in the isospin sector because the nucleonic DDRH parameters also were derived from the Bonn-*A* potential [25]. Because the DB interactions include highly nonlinear and nonperturbative correlation effects the quark model reduction factor $R_q = 2/3$ is not expected to be adequate for hypernuclear structure studies.

Clearly, the final decision on the permissible (R_σ, R_ω) pairs is obtained from a comparison to data. In Fig. 1 the χ^2 deviations of calculated and measured Λ single particle spectra are shown. Varying freely the R_σ and R_ω scaling factors, DDRH single particle energies for $^{208}_{\Lambda}$Pb, $^{89}_{\Lambda}$Y, $^{51}_{\Lambda}$V, $^{40}_{\Lambda}$Ca, $^{28}_{\Lambda}$Si, $^{16}_{\Lambda}$O, $^{12}_{\Lambda}$C, and $^{9}_{\Lambda}$Be were compared to data deduced from (π,K) [40–44] experiments. With precise measurements resolving spin-orbit doublets to high accuracy such a procedure would, in fact, allow us to fix both the scalar and vector scaling factors unambiguously because the centroid and splitting energies are determined by the difference and sum of the scalar and vector mean-field components, respectively.

Unfortunately, under the present experimental conditions doublets are not resolved energetically. Typically, spin-orbit splittings are deduced rather indirectly, e.g., by a line shape analysis [45] which only allows us to set constraints on the energy splitting of spin-orbit partners. The consequences of these experimental uncertainties for a theoretical analysis are clearly seen in Fig. 1: The χ^2 distribution is characterized by a sharp deep valley, which is already known from Refs. [8,16]. The valley extends between $(R_\sigma, R_\omega) = (0.1, 0.1)$ and $(R_\sigma, R_\omega) = (0.8, 0.9)$ and any (R_σ, R_ω) pair in this region would describe the data almost equally well. The quark model value pair $R_\sigma = R_\omega = R_q$ ($R_q = \frac{2}{3}$) is seen to be located at the ridge of the valley. These results clearly illustrate the necessity of high resolution measurements which may become possible in the near future with a new generation of detection systems.

The best known case is probably the $(1p_{3/2}, 1p_{1/2})$ splitting in $^{13}_{\Lambda}$C. A single data point is available from measure-

ments at Brookhaven in 1981 [45] from which $\Delta E = (0.36 \pm 0.3)$ MeV was deduced. In the χ^2 procedure this constraint only excludes extreme values of R_σ and R_ω that are already ruled out by the systematics of hyperon binding energies (see also Sec. IV C) anyway. Despite the large uncertainties the data seem to favor a small Λ spin-orbit splitting. Very recent measurements at AGS/E929 [46] apparently confirm this conclusion.

In order to remain as close as possible to the microscopic DDRH picture we use

$$R_\sigma = 0.490, \qquad (39)$$

which was extracted by Haidenbauer *et al.* [31] for a sharp σ meson of mass $m_\sigma = 550$ MeV. Because in [18,31] the scalar meson channels were described by the correlated exchange of pion and kaon pairs the scalar coupling also includes admixtures of a $\sigma_s \sim s\bar{s}$ field as relevant for the Λ couplings. Since theoretical values for the ω vertex are not available R_ω is treated as a phenomenological parameter. From Fig. 1 and the above value of R_σ one finds immediately

$$R_\omega = 0.553. \qquad (40)$$

In a constant coupling RMF model by Ma *et al.* [30] for the same value of R_σ a relative ω coupling $R_\omega = 0.512$ was obtained. Considering the quite different DDRH interaction structure the deviation is only apparent and, in fact, a surprisingly good agreement can be stated. Moreover, our relative couplings are also consistent with bounds on hyperon-nucleon couplings extracted from neutron star models [9,47].

Very likely, most of the deviations of R_σ and R_ω to the quark model value of 2/3 are caused by the highly nonlinear contributions from the dynamically generated σ and σ_s exchange channel in [18,31]. These genuine many-body effects superimpose additional contributions from the explicit $SU(3)_f$ symmetry breaking and $\omega - \phi$ octet-singlet mixing on the fundamental strong interaction level. Obviously, all these effects cooperate in the same direction, namely to produce deviations from the limiting values predicted by exact $SU(3)$ symmetry. Apparently, the attempt to represent the rather involved dynamics of the scalar channel by a single meson of sharp mass implies an effective vector field of compensating repulsive strength. As a consequence, neither of them can be expected to resemble the properties of the respective bare physical meson.

In $SU(3)$-symmetric models explicit symmetry breaking must be introduced in order to reproduce hypernuclear spectra, e.g., by a symmetry breaking term in the Lagrangian of in the generalized chiral $SU(3)$ σ-model [12] or by means of vertex scaling factors as in the quark-meson-coupling (QMC) model [6]. Because of the close similarity of the QMC and our approach it is instructive to compare to the results of Ref. [6]: For $R_\sigma = R_q$, R_ω has to be rescaled by a factor of 0.93, while $R_\omega = R_q$ requires us to multiply R_σ by 1.10. As can be extracted easily from Fig. 1, for $R_\sigma = R_q$ we would get $R_\omega = R_q \times 0.97$, and, *vice versa*, for $R_\omega = R_q$ we find $R_\sigma = R_q \times 1.15$. A specialty of the QMC is a tensor-

TABLE I. Model parameters of the density dependent Λ–nucleon model.

			$i=N$	$i=\Lambda$
m_N	939.0 MeV	$\dfrac{g^2_{\sigma ii}(\rho=0)}{4\pi}$	26.027	6.249
m_Λ	1115.0 MeV	$\dfrac{g^2_{\sigma ii}(\rho=\rho_0)}{4\pi}$	6.781	1.628
m_σ	550.0 MeV	$\dfrac{g^2_{\omega ii}(\rho=0)}{4\pi}$	40.240	12.287
m_ω	782.6 MeV	$\dfrac{g^2_{\omega ii}(\rho=\rho_0)}{4\pi}$	9.899	3.022
m_ρ	770.0 MeV	$\dfrac{g^2_{\rho ii}}{4\pi}$	1.298	0.000

coupling term arising from the quark-structure of the baryons which keeps the Λ spin-orbit splitting extremely small although the $SU(3)$ couplings are rather large.

IV. RELATIVISTIC HARTREE DESCRIPTION OF SINGLE Λ HYPERNUCLEI

Relativistic DDRH Hartree theory and applications to isospin nuclei were discussed in great detail in Ref. [25] and the references therein. Here, we present DDRH results only for single Λ hypernuclei. The numerical realization follows closely Ref. [25], namely the meson fields are described by Eqs. (31)–(33) and baryonic wave functions are obtained from Eq. (34). The nucleon-meson coupling functionals are those of [39]. The model parameters are compiled in Table I.

A. Density dependent Λ vertices in finite nuclei

Numerically, DDRH calculations rely on baryon-meson vertices taken from infinite matter DB interactions which are applied to finite nuclei in local density approximation (LDA). The success of DDRH theory in describing isospin nuclei is closely related to the saturation properties of nuclear densities from which it is clear that infinite matter conditions are approached gradually with increasing mass
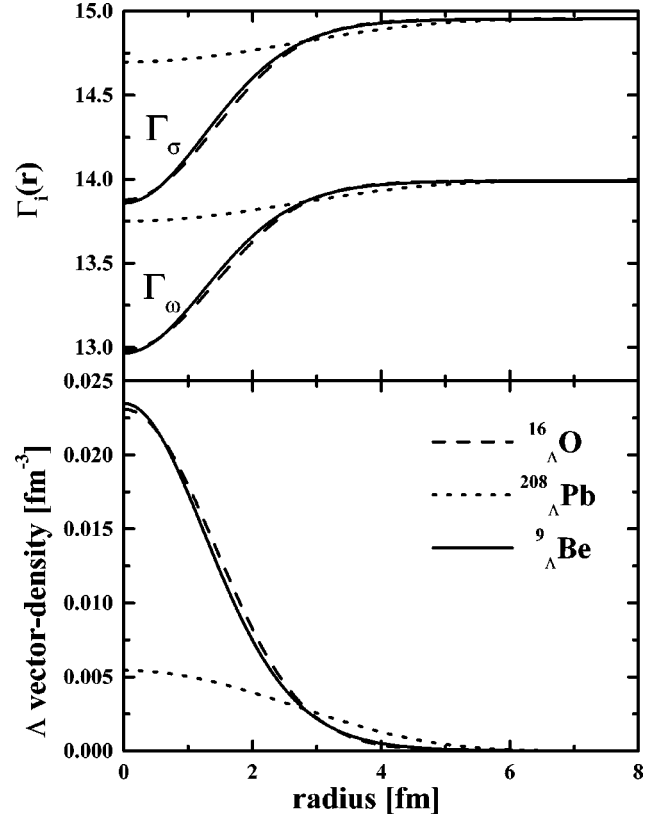

FIG. 2. The radial variation of the DDRH Λ-meson vertices $\Gamma_{\sigma,\omega}$ (upper graph) and of the vector densities (lower graph) for $1s_{1/2}$ Λ states in light and heavy nuclei. Results for the single Λ hypernuclei $^{208}_{\Lambda}$Pb (solid line), $^{16}_{\Lambda}$O (short-dashed line), and $^{9}_{\Lambda}$Be (long-dashed line) are displayed.

number. Under such conditions the LDA is likely to be a rather reliable approach. For light nuclei or, as in single Λ nuclei, small fractions of a specific baryon species with respect to the bulk components effects from the finite size and finite particle number could limit the applicability.

The variation in the effective coupling strengths over the mass table is illustrated in the upper graph of Fig. 2 for the single Λ hypernuclei $^{9}_{\Lambda}$Be, $^{16}_{\Lambda}$O, and $^{208}_{\Lambda}$Pb. The lower graph of Fig. 2 displays the vector densities for $1s_{1/2}\Lambda$ states. In the

TABLE II. Comparison of the Λ and neutron central and central rearrangement potential depths for single Λ hypernuclei.

	$^{208}_{\Lambda}$Pb		$^{89}_{\Lambda}$Y	
	Λ	N	Λ	N
Central	−31.7 MeV	−81.5 MeV	−31.8 MeV	−85.3 MeV
Central rearrangement	1.4 MeV	9.3 MeV	2.0 MeV	8.6 MeV
Σ	−30.3 MeV	−72.2 MeV	−29.8 MeV	−76.7 MeV

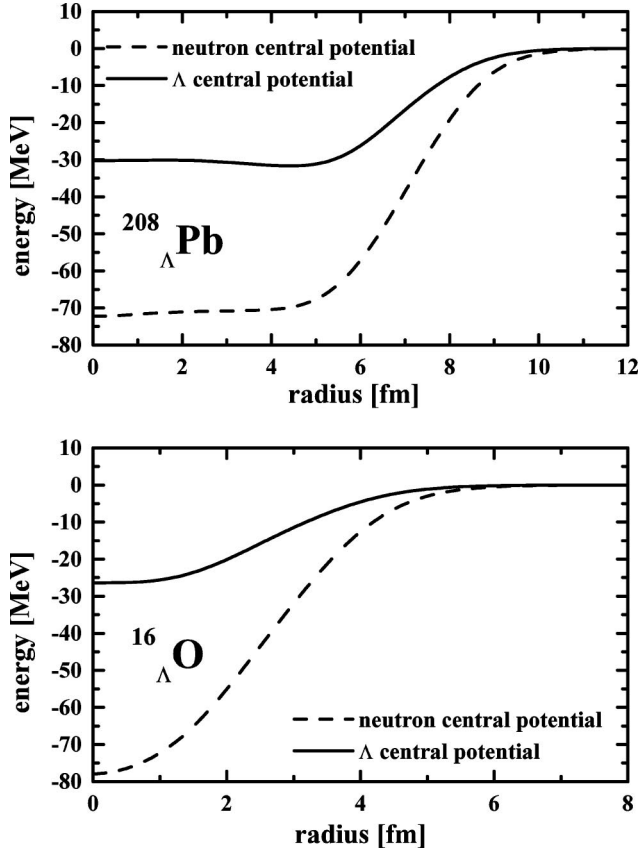|	$^{40}_{\Lambda}$Ca		$^{16}_{\Lambda}$O	
	Λ	N	Λ	N
Central	−31.6 MeV	−90.6 MeV	−28.9 MeV	−86.5 MeV
Central rearrangement	2.3 MeV	10.1 MeV	2.5 MeV	8.6 MeV
Σ	−29.3 MeV	−80.5 MeV	−26.4 MeV	−77.9 MeV

FIG. 3. Comparison of the Schrödinger-equivalent Λ and neutron central potentials including rearrangement. Results for $^{208}_{\Lambda}$Pb and $^{16}_{\Lambda}$O are shown in the upper and lower part of the figure, respectively. The Λ and neutron potentials are of a similar shape but different depth.

TABLE III. The rms radii of the first orbital momentum states for Λ's, neutrons, and protons in $^{40}_{\Lambda}$Ca and $^{208}_{\Lambda}$Pb.

| | $^{40}_{\Lambda}$Ca | | | $^{208}_{\Lambda}$Pb | | |
	Λ	n	p	Λ	n	p
$1s_{1/2}$	2.8 fm	2.3 fm	2.4 fm	4.1 fm	3.8 fm	3.9 fm
$1p_{3/2}$	3.5 fm	3.0 fm	3.0 fm	4.8 fm	4.5 fm	4.6 fm
$1p_{1/2}$	3.6 fm	3.0 fm	3.0 fm	4.7 fm	4.4 fm	4.5 fm
$1d_{5/2}$	4.7 fm	3.5 fm	3.6 fm	5.3 fm	5.0 fm	5.1 fm
$1d_{3/2}$	6.3 fm	3.6 fm	3.7 fm	5.2 fm	4.9 fm	5.0 fm

the difference and (the gradient of) the sum of the relativistic scalar and vector mean fields for the central and the spin-orbit potentials, respectively [25].

It is obvious that the scalar and vector fields scale according to the Λ-meson coupling. Similar to other approaches and in agreement with empirical analyses the Schrödinger-type DDRH Λ-nucleus potential is reduced by a factor of 0.35 to 0.4 compared to the nucleon potential. Results are displayed in Table II and Fig. 3. Since binding energies are reduced accordingly already the wave functions of the deepest bound Λ states are spread over a large part of the nuclear volume resulting in a sensitivity to the complete surrounding density structure. Table III, showing the rms radii of Λ, neutron, and proton states in the hypernuclei $^{40}_{\Lambda}$Ca and $^{208}_{\Lambda}$Pb, illustrates this effect. In Fig. 4 the conventional central and the rearrangement central Λ potentials for light to heavy nuclei are displayed. It is clearly seen that the rearrangement polarization effects are most important in the surface dominated light nuclei. Still, the rearrangement self-energies play only a minor role for single Λ hypernuclei since they are weighted by the Λ vector density [see Eqs. (21), (22)] which is obviously fairly small. The more important effect of the density dependent treatment arises in hypernuclei through the nuclear core creating the Λ's mean-field potentials. The density dependence of the nucleon vertices modifies the core
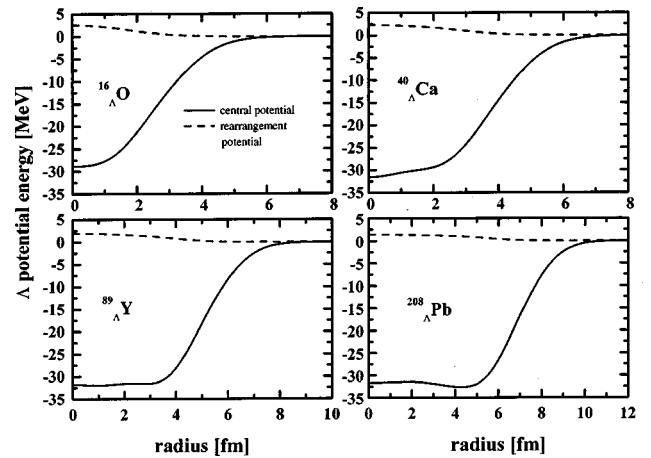
light nuclei the coupling decreases rapidly towards the nuclear center while in lead the DDRH vertices are almost constant. The behavior follows closely the density distributions of the $1s$ Λ states. Their radial extensions are determined by the size of the mean field produced by the nuclear core. Of particular interest is the variation of the vertex functionals with nuclear mass. Apparently, the global density dependence of the infinite matter DB couplings transforms in finite nuclei effectively into a pronounced mass number dependence of the DDRH vertices. From these results it is clear that a complete test of the medium dependence is only obtained in calculations over a wide mass range. Light hypernuclei will be most appropriate to study those vertex parts depending explicitly on the density while heavy nuclei mainly provide information on hyperon interactions at a saturated density. This also points to possible limitations of the present model: the use of LDA vertices may lead to uncertainties in light nuclei where a particular sensitivity on the transition to free space conditions appears.

B. Structure of the Λ mean-field

An appropriate way to understand hypernuclear dynamics and to compare to other calculations is to consider the Schrödinger-equivalent potentials given in lowest order by

FIG. 4. Mean-field potentials for single Λ hypernuclei. The lowest order Schrödinger-equivalent conventional potential (solid line) and rearrangement potential (dashed line) are shown. It is clearly seen that the polarization effects described effectively by the rearrangement potential are most important for light nuclei.
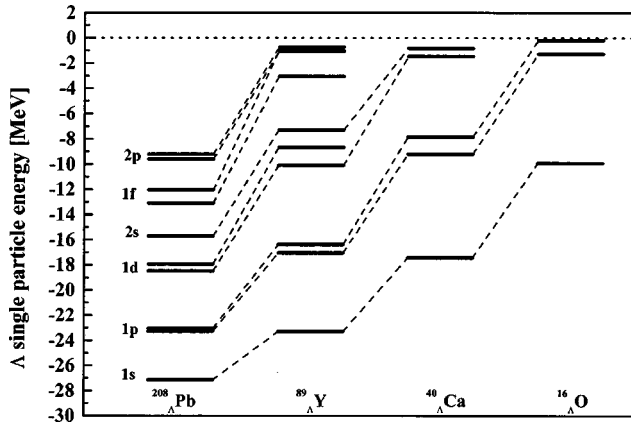
FIG. 5. DDRH Λ single particle spectra in light to heavy hypernuclei.

density distribution over the whole nuclear volume [25], thereby directly affecting the Λ mean field. Since the potential shape and strength is reflected in single particle energies and wave functions a Λ acts as an external probe providing a global measure of the core properties.

C. Single particle states

Hyperon single particle spectra for $|S|=1$ hypernuclei can be seen as a very clean fingerprint of this nucleus, since, as discussed in the last section, they are almost undisturbed by many-body effects. Besides the bulk structure, which contains information on the mean field, i.e., the nucleonic density distribution, the spectra yield information also on other correlations of the baryonic interaction, carried by the fine structure.

Λ and neutron single particle levels for light to heavy nuclei are compared in Figs. 5 and 6. Two major differences between the nucleonic and the Λ spectrum are detected:

(1) Λ and neutron single particle spectra are overall related by a constant shift and an additional quenching factor because the Λ central potential has a depth of only about -30 MeV, compared to -70 MeV for the neutrons (see also Fig. 3 and Table II).
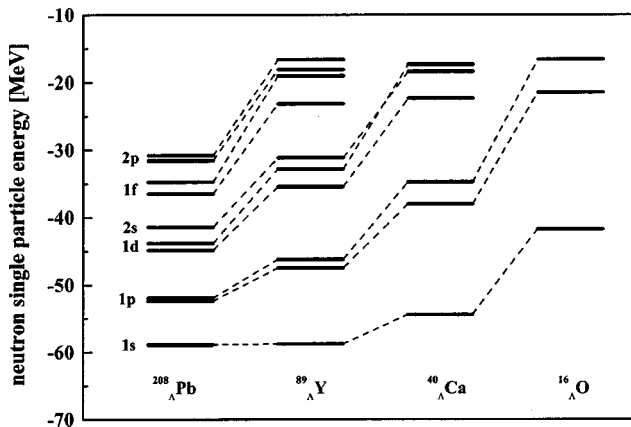

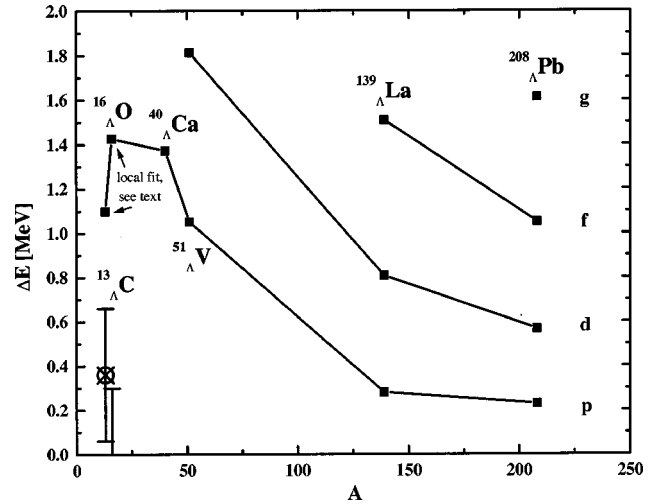FIG. 6. DDRH neutron single particle spectra in light to heavy hypernuclei.

FIG. 7. Dependence of the spin-orbit splitting for $1p_{3/2,1/2}$, $1d_{5/2,3/2}$, $1f_{7/2,5/2}$, $1g_{9/2,7/2}$, and $1h_{11/2,9/2}$ Λ states on nuclear mass. The only available data point [45] for the $1p_{3/2,1/2}$ doublet in $^{13}_{\Lambda}$C and an upper limit for the $1p_{3/2,1/2}$ doublet in $^{16}_{\Lambda}$O [48] is also shown (see Sec. III C).

(2) The spin-orbit splitting of the Λ states is reduced further to less than is expected from the overall quenching of the potential strength.

The reason for the smaller spin-orbit splitting is understood by considering the evolution with increasing mass number. In Fig. 7 the spin-orbit splitting of Λ states for several nuclei across the whole mass range is shown. It can be seen clearly that the splitting drops as expected for higher masses since it has to go to zero in the nuclear matter limit. The splitting also drops in the low mass region, since the spin-orbit doublets approach the continuum threshold and get compressed before one of them or both become unbound. This is a remarkable similarity to the situation found in weakly bound neutron-rich exotic nuclei [49].

For exactly this reason the data point of the $^{13}_{\Lambda}$C $1p$ shell splitting is, though the absolute error is not that large, only of little use to further constrain the relative coupling R_{ω} (see Sec. III C). Because the low mass hypernuclei are systematically underbound with our standard choice for $R_{\sigma,\omega}$ the spin-orbit splittings for $^{13}_{\Lambda}$C and $^{16}_{\Lambda}$O are determined with a readjusted $R_{\omega}=0.542$.[1] Since the spin-orbit splitting data come from a different measurement than the separation energies of Fig. 8, to which R_{ω} was adjusted, a somewhat larger deviation is found. Attempts to reproduce the $^{13}_{\Lambda}$C Λ-$1p$ shell splitting resulted in unrealistically small values of R_{σ} and R_{ω}.

The explanation of the spin-orbit quenching is actually found in the overlap of the Λ single particle wave functions and the spin-orbit potential. As seen from binding energies and confirmed by the rms radii of Λ states shown in Table III and Fig. 9 they are much less localized than nucleonic states

---

[1]With this slightly modified $R_{\omega}=0.542$ the spectra of the low mass hypernuclei are actually nicely described; See Sec. IV D and Fig. 8.
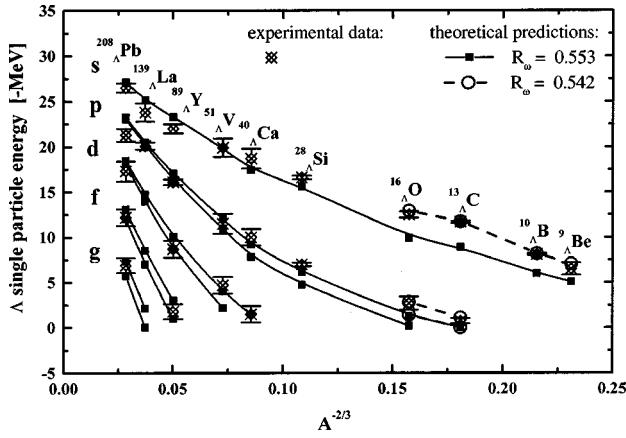
FIG. 8. Comparison of DDRH and experimental single particle energies. The lines are drawn to guide the eye. Results for $R_\omega = 0.542$ are indicated by a dashed line. In order to remove finite size and, especially, surface effects, the energies are shown as a function of $A^{-2/3}$. For $A \to \infty$ they converge asymptotically to the binding energy of a single Λ in infinite matter, $E_\Lambda = -28$ MeV. The data originate from $^A X(\pi,K)_\Lambda^A X$ reactions [40–44].

in the same nucleus (see also Fig. 10). The spin-orbit potential, on the other hand, has its strongest contribution always in a peak structure at the nuclear surface, as seen in Fig. 9. Hence, the overlap of the delocalized Λ wave functions and
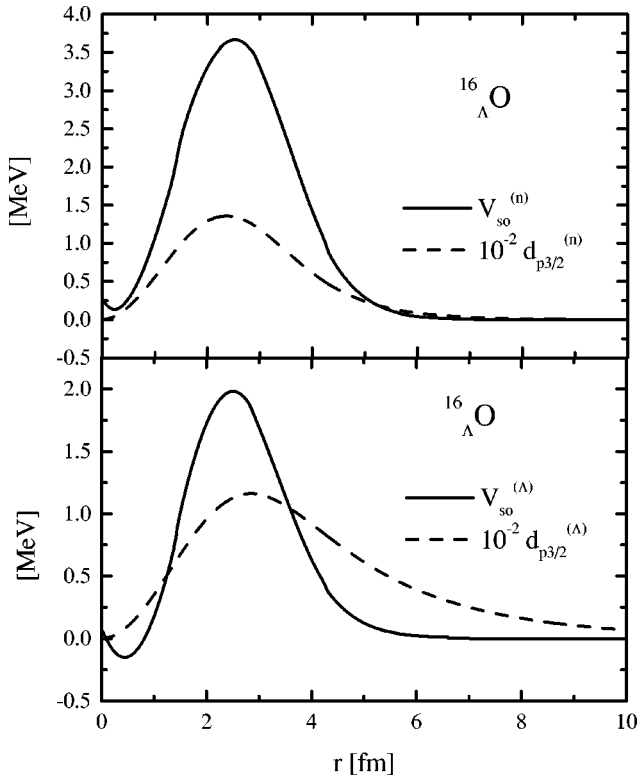

FIG. 9. This figure shows a comparison between the overlap of the Λ $1p_{3/2}$ density $d_{p3/2}^{(\Lambda)}(r) = r^2 \bar{\Psi}_\Lambda \Psi_\Lambda \hbar c$ with its (lowest order Schrödinger equivalent) spin-orbit potential $V_{so}^{(\Lambda)}$ and the respective potential for the neutron in the hypernucleus $_\Lambda^{16}$O. The Λ spin-orbit interaction is, in addition to the smaller spin-orbit potential, reduced due to its delocalization compared to the neutron.
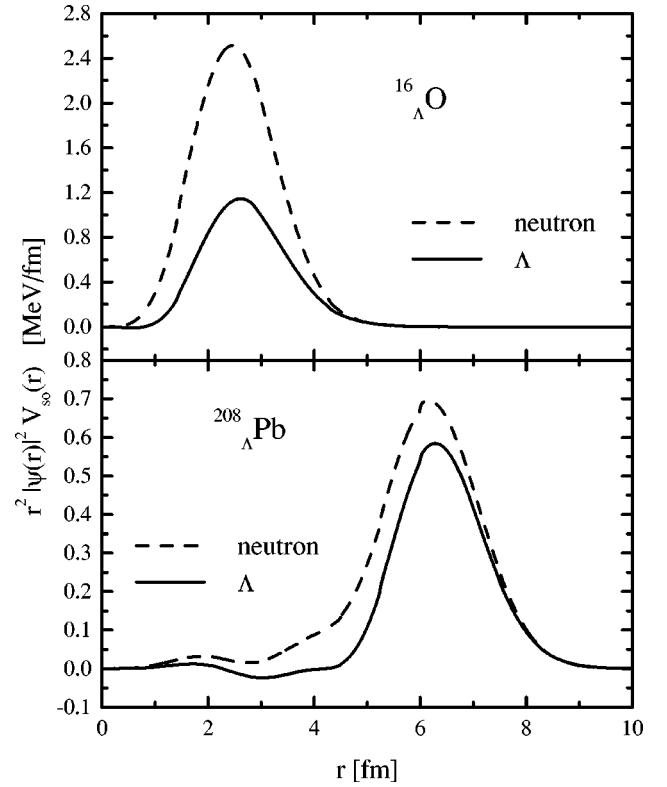

FIG. 10. The integrand of the spin-orbit energy, i.e., the product of the two functions presented in Fig. 9, is shown in this plot for the neutron and the Λ $1p$ states in $_\Lambda^{16}$O and $_\Lambda^{208}$Pb, respectively. It is seen that the reduction of the spin-orbit energy due to the delocalization of the Λ is of special relevance for lower mass nuclei.

the rather sharply localized spin-orbit potential is considerably less than for the stronger bound nucleonic wave functions; Fig. 9 illustrates this. As a result, a much smaller overlap integral and a reduced spin-orbit interaction energy are obtained for Λ states. As seen from Fig. 7 the calculated spin-orbit splitting is still larger than experimental results require. This supports an additional mechanism of reduction. Presumably, this is related to the quark structure of the Λ, indicating for example a tensor coupling to the ω meson [4–6]. The effect of the Λ spin-orbit potential is largest in the low angular momentum doublets of small hypernuclei. Therefore the ideal nuclei to observe spin-orbit potential effects experimentally are those that are heavy enough to bind the $1p$ doublet just without a too large "close-to-threshold squeezing." This can be seen from Fig. 7 to be the region around calcium.

D. Systematics of single Λ states

In Fig. 8 the DDRH single particle spectra are compared to spectroscopic data from (π^+, K^+) reactions. States in intermediate to high mass nuclei are described fairly well by the model, while for masses below about $_\Lambda^{28}$Si deviations to the experimental data of up to 2.5 MeV arise. As discussed in Sec. IV A, in this mass region the limits of using LDA vertices may be approached. We seem to overestimate systematically the strength of the repulsive vector interaction in

TABLE IV. Transition energies for (K,π) reactions on a nucleus [50,51]. These states include Λ particle-n hole excitations of the single Λ hypernuclei. The experimental values (expt.) are compared to DDRH and a phenomenological RMF model [8] (phen. RMF) with nonlinear σ self-interactions.

	n valence shell	state	Expt. [MeV]	DDRH [MeV]	Phen. RMF [MeV]
$^{12}_{\Lambda}$C	$1p_{3/2}$	$(1s_{1/2}\Lambda, 1p_{3/2}n^{-1})$	6.72 ± 2	6.69	5.02
		$(1p_{3/2}\Lambda, 1p_{3/2}n^{-1})$	18.48 ± 2	15.11	17.21
$^{16}_{\Lambda}$O	$1p_{1/2}$	$(1s_{1/2}\Lambda, 1p_{1/2}n^{-1})$	3.35 ± 2	5.76	3.53
		$(1s_{1/2}\Lambda, 1p_{3/2}n^{-1})$	9.90 ± 2	10.13	9.46
		$(1p_{1/2}\Lambda, 1p_{1/2}n^{-1})$	13.20 ± 2	16.16	13.89
		$(1p_{3/2}\Lambda, 1p_{3/2}n^{-1})$	19.20 ± 2	18.40	18.88
$^{40}_{\Lambda}$Ca	$1d_{3/2}$	$(1p_{1/2}\Lambda, 1d_{3/2}n^{-1})$	5.79 ± 2	8.84	7.40
		$(1d_{3/2}\Lambda, 1d_{3/2}n^{-1})$	14.47 ± 2	11.34	15.48
		$(1d_{5/2}\Lambda, 1d_{5/2}n^{-1})$	19.35 ± 2	20.07	20.71

low mass single Λ hypernuclei. This tendency already becomes apparent in going from $^{51}_{\Lambda}$V to $^{28}_{\Lambda}$Si. In Fig. 8 results of a calculation are included in which the vector scaling factor was slightly decreased by about 2% to $R_{\omega}=0.542$. Figure 1 shows that this value is also located in the valley of the χ^2 distribution. The Λ separation energies in the light mass nuclei are well reproduced but the agreement in the high mass region would deteriorate. The result indicates the sensitivity of the DDRH calculations on fine details of the interplay of scalar attraction and vector repulsion. Clearly, under the present conditions a 2% variation is well within the uncertainties of the model and, moreover, may be taken to indicate a typical boundary for the validity of LDA in light mass nuclei.

For the heavier nuclei the microscopic DDRH results are of a quality which is at least comparable to the phenomenological descriptions. This we consider as a remarkable success for a model which essentially contains only a single free parameter, namely the overall vector vertex scaling factor R_{ω}.

Finally, we will look at (K^-,π^-) data measured at the end of the 1970's at CERN [50,51]. This data set was not included in the determination of R_{ω} because of its relatively large error bars. Table IV shows these data together with the DDRH predictions and phenomenological RMF [8] calculations. These data contain besides Λ single particle states also information on the energies of Λ-particle neutron-hole states. These were calculated approximately within the Hartree scheme by keeping a neutron hole at the specified place during the iteration. A more realistic calculation would require us to perform a complete RPA calculation which is, however, at present neither feasible nor worthwhile. A further complication in modeling these nuclei is the relatively small mass numbers, as discussed already above. Taking into account the fairly low energy resolution of the data and keeping in mind the previously discussed subtleties the (K,π) data are also described satisfactorily well on a level comparable to phenomenological RMF models.

V. SUMMARY AND CONCLUSION

The DDRH theory introduced previously for neutron and proton isospin nuclei was extended to hypernuclei by including the full set of $SU(3)_f$ octet baryons. Interactions were described by a model Lagrangian including strangeness-neutral scalar and vector meson fields of $q\bar{q}$ ($q=u,d$) and $s\bar{s}$ quark character. The medium dependence of interactions was described by meson-baryon vertices chosen as functionals of the baryon field operators. Following DDRH theory their structure is determined such that interaction diagrams contributing nonperturbatively to the ground-state energies and wave functions are cancelled. Here, the DDRH vertices were chosen to cancel Dirac-Brueckner ground-state correlations. Hence, the approach corresponds to a resummation of ladder diagrams into the vertices under the constraint that infinite matter ground-state self-energies and total binding energies are reproduced. As the central theoretical result it was found that the structure of Dirac-Brueckner interactions strongly indicates that the ratio of nucleon and hyperon in-medium vertices should be determined already by the ratio of the corresponding free space coupling constants being affected only weakly by the background medium. Apparently, the presently available hypernuclear data are, at least, not contradicting such a scaling law.

Dynamical scaling will have several important consequences for hypernuclear investigations. First of all, it might be considered to give a sound theoretical support to the general conviction that hypernuclei are suitable to gain information on octet dynamics. A conclusion of equal importance is that hypernuclei should follow essentially the same rules as isospin nuclei except for a shift of energy scales. A point worth investigating in more detail in the future is whether hypernuclear scaling might provide a way to study the dynamical evolution of $SU(3)$ flavor symmetry in a medium.

In order to test dynamical scaling, RMF calculations for single Λ hypernuclei were performed. Using the previously derived meson-nucleon vertices [25] and fixing the $\sigma\Lambda$ vertex by a theoretical value from the literature [18,31] the ω meson-Λ vertex scaling factor was determined by a least squares fit procedure, thus determining the only free parameter of the model empirically from a selected set of data. Calculations over the full range of known single Λ nuclei led to a very satisfactory description of Λ separation energies. The deviations from the overall agreement for masses below

$A \approx 16$ are probably related to the enhancement of surface effects in light nuclei. Very likely, they indicate the limitations of static RMF calculations with DB vertices obtained in the local density approximation. The minor adjustment of parameters, necessary to achieve agreement also for the light mass systems, indicates the sensitivity of these surface-dominated nuclei on dynamical details. In a recent nonrelativistic calculation indeed sizable contributions of hyperon polarization self-energies especially in light nuclei [52] were found.

The results are encouraging and we conclude that DDRH theory, extended to the strangeness sector, is in fact an appropriate basis for a microscopic treatment of hypernuclei.

The present formulation and applications are first steps on the way to a more general theory of in-medium $SU(3)_f$ flavor dynamics. Future progress on dynamical scaling and other theoretical aspects of the approach will depend on the availability of Dirac-Brueckner calculations for the full baryon octet including also the complete pseudoscalar 0^- and vector 1^+ meson multiplets.

ACKNOWLEDGMENT

[1] H. Bandō, T. Motoba, and J. Zofka, Int. J. Mod. Phys. A **5**, 4021 (1990).

[2] R. E. Chrien and C. B. Dover, Annu. Rev. Nucl. Part. Sci. **39**, 151 (1989).

[3] B. K. Jennings, Phys. Lett. B **246**, 691 (1990).

[4] M. Chiapparini, A. O. Gattone, and B. K. Jennings, Nucl. Phys. **A529**, 589 (1991).

[5] J. Mares and B. K. Jennings, Phys. Rev. C **49**, 2472 (1994).

[6] K. Tsushima, K. Saito, J. Haidenbauer, and A. W. Thomas, Nucl. Phys. **A630**, 691 (1998).

[7] B. D. Serot and J. D. Walecka, *Advances of Nuclear Physics*, edited by J. W. Negele and E. Vogt (Plenum, New York, 1986), Vol. 16, p. 1; J. D. Walecka, Ann. Phys. (N.Y.) **83**, 497 (1974).

[8] M. Rufa, J. Schaffner, J. Maruhn, H. Stöcker, and W. Greiner, Phys. Rev. C **42**, 2469 (1990).

[9] N. K. Glendenning, D. Von-Eiff, M. Haft, H. Lenske, and M. K. Weigel, Phys. Rev. C **48**, 889 (1993).

[10] D. Vretenar, P. Pöschl, G. A. Lalazissis, and P. Ring, Phys. Rev. C **57**, 1060 (1998).

[11] H. Müller, Phys. Rev. C **59**, 1405 (1999).

[12] P. Papazoglou, D. Zschiesche, S. Schramm, J. Schaffner-Bielich, H. Stöcker, and W. Greiner, Phys. Rev. C **59**, 411 (1999); P. Papazoglou, S. Schramm, J. Schaffner-Bielich, H. Stöcker, and W. Greiner, *ibid.* **57**, 2576 (1998).

[13] K. Tsushima, K. Saito, and A. W. Thomas, Phys. Lett. B **411**, 9 (1997).

[14] C. Greiner and J. Schaffner, Int. J. Mod. Phys. E **5**, 239 (1996); J. Schaffner, C. B. Dover, A. Gal, C. Greiner, D. J. Millener, and H. Stöcker, Ann. Phys. (N.Y.) **235**, 35 (1994); J. Schaffner, C. B. Dover, A. Gal, C. Greiner, and H. Stöcker, Phys. Rev. Lett. **71**, 1328 (1993); J. Schaffner, C. Greiner, and H. Stöcker, Phys. Rev. C **46**, 322 (1992).

[15] M. Rufa, H. Stocker, J. A. Maruhn, W. Greiner, and P. G. Reinhard, J. Phys. G **13**, L143 (1987).

[16] J. Mares and J. Zofka, Z. Phys. A **333**, 209 (1989).

[17] C. Greiner, P. Koch, and H. Stöcker, Phys. Rev. Lett. **58**, 1825 (1987).

[18] A. Reuber, K. Holinde, H.-C. Kim, and J. Speth, Nucl. Phys. **A608**, 243 (1996).

[19] V. G. J. Stoks and Th. A. Rijken, Phys. Rev. C **59**, 3009 (1999).

[20] Th. A. Rijken, V. G. J. Stoks, and Y. Yamamoto, Phys. Rev. C **59**, 21 (1999).

[21] V. G. J. Stoks and T.-S. H. Lee, Phys. Rev. C **60**, 024006 (1999).

[22] I. Vidana, A. Polls, A. Ramos, M. Hjorth-Jensen, and V. G. Stoks, Phys. Rev. C **61**, 025802 (2000).

[23] H.-J. Schulze, M. Baldo, U. Lombardo, J. Cugnon, and A. Lejeune, Phys. Rev. C **57**, 704 (1998).

[24] H. Lenske and C. Fuchs, Phys. Lett. B **345**, 355 (1995).

[25] C. Fuchs, H. Lenske, and H. Wolter, Phys. Rev. C **52**, 3043 (1995).

[26] J. W. Negele, Rev. Mod. Phys. **54**, 913 (1982).

[27] Y. K. Gambhir, P. Ring, and A. Thimet, Ann. Phys. (N.Y.) **198**, 132 (1990); P.-G. Reinhard, M. Rufa, J. Maruhn, W. Greiner, and J. Friedrich, Z. Phys. A **323**, 13 (1986).

[28] F. de Jong and H. Lenske, Phys. Rev. C **57**, 3099 (1998).

[29] F. de Jong and H. Lenske, Phys. Rev. C **58**, 890 (1998).

[30] Zhong-Yu Ma, J. Speth, S. Krewald, and Bao-Qiu Chen, Nucl. Phys. **A608**, 305 (1996).

[31] J. Haidenbauer, W. Melnitchouk, and J. Speth, Proceedings of SENDAI 98, nucl-th/9805014.

[32] Ta-Pei Cheng and Ling-Fong Li, *Gauge Theory of Elementary Particle Physics* (Clarendon, Oxford, 1991).

[33] S. Marcos, R. J. Lombard, and J. Mares, Phys. Rev. C **57**, 1178 (1998).

[34] C. J. Horowitz and B. D. Serot, Nucl. Phys. **A399**, 529 (1983).

[35] C. J. Horowitz and B. D. Serot, Nucl. Phys. **A464**, 613 (1987).

[36] B. ter Haar and R. Malfliet, Phys. Rep. **149**, 207 (1987).

[37] J. D. Bjorken and S. D. Drell, *Relativistic Quantum Fields* (McGraw-Hill, New York, 1965).

[38] S. Haddad and M. Weigel, Phys. Rev. C **48**, 2740 (1993).

[39] R. Brockmann and R. Machleidt, Phys. Rev. C **42**, 1965 (1990).

[40] T. Hasegawa *et al.*, Phys. Rev. C **53**, 1210 (1996).

[41] S. Ajimura *et al.*, Nucl. Phys. **A585**, 173c (1995).

[42] P. H. Pile *et al.*, Phys. Rev. Lett. **66**, 2585 (1991).

[43] D. H. Davis and J. Pniewski, Contemp. Phys. **27**, 91 (1986).

[44] M. May *et al.*, Phys. Rev. Lett. **78**, 4343 (1997).

[45] M. May *et al.*, Phys. Rev. Lett. **47**, 1106 (1981).

[46] A. Sakaguchi for the AGS/E929 Collaboration, *Proceedings of SNP' 99*, Seoul (World Scientific, Singapore, 1999).

[47] H. Huber, K. Weigel, and F. Weber, Z. Naturforsch., A: Phys. Sci. **54**, 77 (1999).

[48] W. Brückner *et al.*, Phys. Lett. **79B**, 157 (1978).

[49] H. Lenske, J. Phys. G **24**, 1429 (1998).

[50] B. Povh, Nucl. Phys. **A335**, 233 (1980).

[51] R. Bertini *et al.*, Phys. Lett. **83B**, 306 (1979).

[52] I. Vidaña, A. Polls, A. Ramos, and M. Hjorth-Jensen, nucl-th/9809060; I. Vidaña, A. Polls, A. Ramos, and M. Hjorth-Jensen, Nucl. Phys. **A644**, 201 (1998).